DALTON
FULL PAPER

Synthesis, structure, luminescence and electrochemical studies of a novel class of ruthenium(II) polypyridine complexes with ortho-metallated aminocarbene ligands

Vivian Wing-Wah Yam,* Ben Wai-Kin Chu, Chi-Chiu Ko and Kung-Kai Cheung

Department of Chemistry, The University of Hong Kong, Pokfulam Road, Hong Kong SAR, People's Republic of China. Fax: (852)2857-1586; E-mail: wwyam@hku.hk

Received 18th January 2001, Accepted 12th April 2001
First published as an Advance Article on the web 23rd May 2001

A series of ruthenium(II) orthometallated aminocarbene complexes have been synthesized and characterized. Their electrochemistry, electronic absorption, emission, and the crystal structures of $[\overline{Ru(phen)_2\{=C(CH_2Ph)NHC_6H_4\}}]$-$CF_3SO_3$, $[\overline{Ru(bpy)_2\{=C(CH_2Ph)NMeC_6H_4\}}]PF_6$ and $[\overline{Ru(bpy)_2\{=C(CH_2C_4H_3S)NHC_6H_4\}}]CF_3SO_3$ have been studied. The nature of the electronic transitions and the origin of the emission are discussed and an assignment of a ^{3}MLCT emission has been supported by EHMO studies.

Introduction

Since the first synthesis of a carbene complex the chemistry of Fischer carbene complexes has been developing in an explosive fashion and has become an important branch of organometallic chemistry. The major thrust of this development stems from the synthesis and characterization of hundreds and thousands of related complexes and their use as synthons and catalysts. They have been vastly used in cyclopropanation reactions,[1] olefin metathesis,[2] ring-opening metathesis polymerization (ROMP),[3] ring-closing metathesis (RCM)[4,5] and carbonyl olefination reactions.[1c] This provided a driving force for the rapid development of new areas of organometallic chemistry and a large portion of the research efforts involving carbene, alkene and metallacycle complexes of transition metals is oriented toward understanding these important catalytic sequences. An extremely important and related chemistry is Fischer–Tropsch chemistry,[6] in which both vinylidene and carbene species are thought to be key intermediates in the hydrogenation of CO catalyzed by iron-group metals to give a variety of organic products. While syntheses and studies of ruthenium complexes of these sorts are mainly confined to those containing phosphine ligands,[7] corresponding studies on complexes with nitrogen donor ligands are relatively rare and less extensively explored.[8] In view of the rich photophysical and photochemical behaviour of ruthenium(II) polypyridyl complexes[9] and our recent efforts on luminescent organometallic complexes,[10] the introduction of a polypyridyl moiety to ruthenium(II) carbene complexes is expected to bring rich luminescence behaviour to the organometallic ruthenium carbene species. Recently, we communicated the isolation of a luminescent ruthenium(II) aminocarbene complex of bipyridine.[11] As an extension of our preliminary communication and to provide further insights on the spectral origin of the electronic absorption and emission behaviour, an extensive series of ruthenium(II) orthometallated aminocarbene complexes have been synthesized and characterized. Their electrochemistry, photophysical behaviour, and crystal structures are also reported. Spectral assignments of the electronic absorption and emission origin of these complexes have also been supported by EHMO calculations.

Experimental

Materials and reagents

2,2′-Bipyridine, 1,10-phenanthroline and 4-trifluoromethylaniline were obtained from Lancaster Synthesis Ltd., aniline, anisidine, 4-bromoaniline, 1-chloro-4-ethynylbenzene and phenylacetylene from Aldrich Chemical Co. 2-Ethynylthiophene[12] and the ruthenium(II) starting materials, *cis*-$[Ru(bpy)_2Cl_2]$,[13] and *cis*-$[Ru(phen)_2Cl_2]$,[13] were synthesized according to the literature procedures. Aniline, *N*-methylaniline and phenylacetylene were freshly distilled before use. Acetonitrile (Lab-Scan, AR) was used as obtained for synthesis and distilled over calcium hydride for physical measurements. Tetra-*n*-butylammonium hexafluorophosphate ($^nBu_4NPF_6$) (Aldrich, 98%) was purified by recrystallization from ethanol three times before use. All other reagents were of analytical grade used as received.

General preparation method

All reactions were performed under strictly anaerobic and anhydrous conditions using standard Schlenk techniques. *cis*-$[Ru(bpy)_2Cl_2]\cdot 2H_2O$ (100 mg, 0.19 mmol) and AgOTf (OTf = O_3SCF_3) (100 mg, 0.39 mmol) were mixed and stirred in dry acetone (20 ml) under nitrogen for 3 hours. The solution was filtered to remove the precipitated AgCl and evaporated to dryness. Reaction of *cis*-$[Ru(bpy)_2(Me_2CO)_2][OTf]_2$ with acetylene (A) (0.58 mmol) in the presence of an excess of amine (B) (0.77 mmol) in dry acetone under an inert atmosphere of nitrogen gave a purple solution, which was then filtered and evaporated to dryness under reduced pressure. The product was either obtained as its hexafluorophosphate salt, by adding a saturated methanolic solution of NH_4PF_6 to the complex in methanol, or directly as the trifluoromethanesulfonate salt. The purple solid obtained was recrystallized by vapour diffusion of diethyl ether into an acetonitrile or acetone solution of the product to yield purplish red crystals.

$[\overline{Ru(bpy)_2\{=C(CH_2Ph)NHC_6H_4\}}]PF_6$ 1. A = Phenylacetylene (59 mg, 0.58 mmol); B = aniline (72 mg, 0.77 mmol). The complex has previously been communicated.[11] Yield: 60%.

Elemental analyses, $C_{34}H_{28}F_6N_5PRu$, Calc. (found) (%): C 54.26 (54.22), H 3.75 (3.56), N 9.30 (9.23). ^{1}H NMR (300 MHz, CD_3CN, 298 K): δ 4.3 (s, 2H, CH_2), 6.3 (d, J = 7, 2H, aromatic H), 6.40 (d, J = 6, 1H, aromatic H), 6.6–6.7 (m, 3H, aromatic H), 6.8 (m, 1H, aromatic H), 6.90 (t, J = 7.5, 1H, aromatic H), 7.2 (m, 1H, aromatic H), 7.2–7.3 (m, 5H, aromatic H), 7.6–7.9 (m, 8H, aromatic H), 8.2 (s, 1H, aromatic H), 8.2 (d, J = 6, 1H, aromatic H), 8.3 (d, J = 8 Hz, 1H, aromatic H), 11.3 (s, broad, 1H, NH). ^{13}C NMR (67.8 MHz, CD_3CN, 298 K): δ 52.7 (CH_2), 114.0–176.6 (aromatic C), 266.0 (Ru=C). Positive FAB-MS: m/z 607, $\{M - PF_6\}^+$.

[Ru(bpy)$_2${=C(CH$_2$Ph)NHC$_6$H$_3$OMe}]ClO$_4$ 2. A = Phenylacetylene (59 mg, 0.58 mmol); B = anisidine (95 mg, 0.77 mmol). The complex has previously been communicated.[11] Yield: 70%. Elemental analyses, $C_{35}H_{30}ClN_5O_5Ru$, Calc. (found) (%): C 57.03 (57.24), H 4.10 (4.08), N 9.50 (9.74). ^{1}H NMR (300 MHz, CD_3CN, 298 K): δ 3.5 (s, 3H, OCH_3), 4.3 (s, 2H, CH_2), 5.8 (d, J = 2.5, 1H, aromatic H), 6.2 (d, J = 7, 1H, aromatic H), 6.4 (dd, J = 6, 2.5, 2H, aromatic H), 6.7 (t, J = 6.5, 2H, aromatic H), 6.9 (t, J = 7.5, 1H, aromatic H), 7.2–7.3 (m, 6H, aromatic H), 7.7 (dt, J = 7.5, 1.5, 1H, aromatic H), 7.7–7.9 (m 7H, aromatic H), 8.2–8.3 (m, 2H, aromatic H), 8.3 (d, J = 8 Hz, 1H, aromatic H), 11.2 (s broad, 1H, NH). ^{13}C NMR (125.8 MHz, CD_3CN, 298 K): δ 53.3 (OCH_3), 55.7 (CH_2), 105.9–180.1 (aromatic C), 262.7 (Ru=C). Positive ESI-MS: m/z 638, $\{M - ClO_4\}^+$.

[Ru(phen)$_2${=C(CH$_2$Ph)NHC$_6$H$_4$}]CF$_3$SO$_3$ 3. A = Phenylacetylene (59 mg, 0.58 mmol); B = aniline (72 mg, 0.77 mmol). The complex was synthesized by using *cis*-[Ru(phen)$_2$Cl$_2$] (103 mg, 0.19 mmol) as the starting material instead of *cis*-[Ru(bpy)$_2$Cl$_2$]. Yield: 60%. Elemental analyses, $C_{39}H_{28}F_3N_5O_3RuS$, Calc. (found) (%): C 58.20 (58.22), H 3.51 (3.56), N 8.70 (8.83). ^{1}H NMR (300 MHz, CD_3CN, 298 K), δ 4.4 (m, 2H, CH_2), 5.9 (d, J = 8, 2H, aromatic H), 6.2 (t, J = 8, 2H, aromatic H), 6.3, (d, J = 7, 1H, aromatic H), 6.4 (t, J = 7, 1H, aromatic H), 6.5 (t, J = 7.5, 1H, aromatic H), 6.8 (t, J = 7.5, 1H, aromatic H), 7.3 (d, J = 7, 1H, aromatic H), 7.4 (m, 2H, aromatic H), 7.5 (m, 1H, aromatic H), 7.6 (m, 1H, aromatic H), 7.6 (m, 1H, aromatic H), 7.8 (m, 2H, aromatic H), 8.0 (s, 2H, aromatic H), 8.1 (m, 2H, aromatic H), 8.2 (m, 2H, aromatic H), 8.3 (m, 2H, aromatic H), 8.7 (d, J = 8 Hz, 1H, aromatic H), 11.4 (s, broad, 1H, NH). ^{13}C NMR (125.8 MHz, CD_3CN, 298 K): δ 52.8 (CH_2), 113.5–178.3 (aromatic C), 265.6 (Ru=C). Positive ESI-MS: m/z 656, $\{M - PF_6\}^+$.

[Ru(bpy)$_2${=C(CH$_2$Ph)NMeC$_6$H$_4$}]PF$_6$ 4. A = Phenylacetylene (59 mg, 0.58 mmol); B = *N*-methylaniline (82 mg, 0.77 mmol). Yield: 85%. Elemental analyses, $C_{35}H_{30}F_6N_5PRu$, Calc. (found) (%): C 54.83 (54.60), H 3.94 (4.01), N 9.13 (9.12). ^{1}H NMR (300 MHz, CD_3CN, 298 K): δ 3.9 (s, 3H, NCH_3), 4.6 (d, J = 16, 1H, PhC*H*), 4.8 (d, J = 16, 1H, PhC*H*), 6.0 (d, J = 8, 2H, aromatic H), 6.4 (dd, J = 6, 1, 1H, aromatic H), 6.6 (t, J = 8, 2H, aromatic H), 6.7 (t, J = 7, 1H, aromatic H), 6.8–7.0 (m, 2H, aromatic H), 7.1 (t, J = 7, 1H, aromatic H), 7.2–7.4 (m, 5H, aromatic H), 7.6–7.9 (m, 8H, aromatic H), 8.1 (d, J = 5.5, 1H, aromatic H), 8.2 (d, J = 8, 1H, aromatic H), 8.3 (d, J = 8 Hz, 1H, aromatic H). ^{13}C NMR (125.8 MHz, CD_3CN, 298 K): δ 48.0 (NCH_3), 52.7 (CH_2), 114.2–179.0 (aromatic C), 267.9 (Ru=C). Positive ESI-MS: m/z 622, $\{M - PF_6\}^+$.

[Ru(bpy)$_2${=C(CH$_2$C$_4$H$_3$S)NHC$_6$H$_4$}]CF$_3$SO$_3$ 5. A = 2-Ethynylthiophene (63 mg, 0.58 mmol); B = aniline (72 mg, 0.77 mmol). Yield: 70%. Elemental analyses, $C_{33}H_{26}F_3N_5O_3RuS_2 \cdot CH_3CN$, Calc. (found) (%): C 52.30 (52.25), H 3.64 (3.35), N 10.45 (10.64). ^{1}H NMR (300 MHz, CD_3CN, 298 K): δ 4.4 (m, 2H, CH_2), 5.9 (d, J = 8, 1H, aromatic H), 6.4 (d, J = 6, 1H, aromatic H), 6.5 (m, 1H, aromatic H), 6.6 (m, 1H, aromatic H), 6.8 (m, 1H, aromatic H), 6.9 (d, J = 7, 1H, aromatic H), 7.2–7.9 (m, 12H, aromatic H), 8.0 (d, J = 5.5, 1H, aromatic H), 8.1 (d, J = 7, 1H, aromatic H), 8.2 (d, J = 5, 1H, aromatic H), 8.3 (d, J = 8, 1H, aromatic H), 8.4 (d, J = 8 Hz, 1H, aromatic H), 11.2 (s, broad, 1H, NH). ^{13}C NMR (125.8 MHz, CD_3CN, 298 K): δ 45.8 (CH_2), 114.3–177.0 (aromatic C), 261.9 (Ru=C). Positive ESI-MS: m/z 614, $\{M - PF_6\}^+$.

[Ru(bpy)$_2${=C(CH$_2$Ph)NHC$_6$H$_3$Br}]PF$_6$ 6. A = Phenylacetylene (59 mg, 0.58 mmol); B = 4-bromoaniline (132 mg, 0.77 mmol). Yield: 95%. Elemental analyses, $C_{34}H_{27}BrF_6N_5PRu$, Calc. (found) (%): C 49.11 (49.02), H 3.27 (3.12), N 8.42 (8.16). ^{1}H NMR (300 MHz, CD_3CN, 298 K): δ 4.3 (s, 2H, CH_2), 6.2 (d, J = 8.5, 2H, aromatic H), 6.4 (d, J = 2, 1H, aromatic H), 6.7 (t, J = 7.5, 2H, aromatic H), 6.9 (t, J = 7.5, 1H, aromatic H), 7.0 (dd, J = 6, 2, 1H, aromatic H), 7.1–7.4 (m, 6H, aromatic H), 7.6–8.0 (m, 8H, aromatic H), 8.1 (d, J = 5, 1H, aromatic H), 8.2 (d, J = 8, 1H, aromatic H), 8.3 (d, J = 8 Hz, 1H, aromatic H), 11.3 (s, broad, 1H, NH). ^{13}C NMR (125.8 MHz, CD_3CN, 298 K): δ 52.6 (CH_2), 115.7–182.1 (aromatic C), 267.6 (Ru=C). Positive ESI-MS: m/z 687, $\{M - PF_6\}^+$.

[Ru(bpy)$_2${=C(CH$_2$Ph)NHC$_6$H$_3$CF$_3$}]PF$_6$ 7. A = Phenylacetylene (59 mg, 0.58 mmol); B = 4-trifluoromethylaniline (124 mg, 0.77 mmol). Yield: 50%. Elemental analyses, $C_{35}H_{27}F_9N_5PRu \cdot ¾(CH_3)_2CO$, Calc. (found) (%): C 51.77 (52.12), H 3.67 (3.34), N 8.10 (8.10). ^{1}H NMR (300 MHz, CD_3CN, 298 K): δ 4.2 (s, 2H, CH_2), 6.1 (d, J = 7.5, 2H, aromatic H), 6.6 (m, 3H, aromatic H), 6.8 (t, J = 7.5, 1H, aromatic H), 7.0–7.3 (m, 7H, aromatic H), 7.5 (d, J = 5, 1H, aromatic H), 7.6 (dt, J = 8, 2, 1H, aromatic H), 7.7–7.9 (m, 6H, aromatic H), 8.1 (d, J = 5.5, 1H, aromatic H), 8.2 (d, J = 8, 1H, aromatic H), 8.3 (d, J = 8 Hz, 1H, aromatic H), 11.3 (s, broad, 1H, NH). ^{13}C NMR (125.8 MHz, CD_3CN, 298 K): δ 52.0 (CH_2), 112.4–177.5 (aromatic C), 269.6 (Ru=C). Positive ESI-MS: m/z 676, $\{M - PF_6\}^+$.

[Ru(bpy)$_2${=C(CH$_2$C$_6$H$_4$Cl)NHC$_6$H$_4$}]PF$_6$ 8. A = *p*-Chlorophenylacetylene (79 mg, 0.58 mmol); B = aniline (72 mg, 0.77 mmol). Yield: 65%. Elemental analyses, $C_{34}H_{27}ClF_6N_5PRu$, Calc. (found) (%): C 51.88 (51.83), H 3.46 (3.44), N 8.90 (8.63). ^{1}H NMR (300 MHz, CD_3CN, 298 K): δ 4.3 (q, J = 9, 14, 2H, CH_2), 6.2 (d, J = 8.5, 2H, aromatic H), 6.4 (d, J = 7, 1H, aromatic H), 6.7 (d, J = 8.5, 3H, aromatic H), 6.8 (dt, J = 7.5, 1, aromatic H), 7.1–7.4 (m, 6H, aromatic H), 7.6–8.0 (m, 8H, aromatic H), 8.2 (t, J = 8, 2H, aromatic H), 8.3 (d, J = 8 Hz, 1H, aromatic H), 11.3 (s, broad, 1H, NH). ^{13}C NMR (125.8 MHz, CD_3CN, 298 K): δ 50.9 (CH_2), 113.3–176.0 (aromatic C), 264.6 (Ru=C). Positive ESI-MS: m/z 642, $\{M - PF_6\}^+$.

Physical measurements and instrumentation

Electronic absorption spectra were recorded on a Hewlett-Packard 8452A diode array spectrophotometer, steady state emission and excitation spectra at room temperature and 77 K on a Spex Fluorolog-2 Model F 111 fluorescence spectrophotometer. Solid state photophysical studies were carried out with solid samples contained in a quartz tube inside a quartz walled Dewar flask. Measurements of the EtOH–MeOH (4 : 1, v/v) glass or solid state samples at 77 K were similarly conducted with a liquid nitrogen filled optical Dewar flask. Excited state lifetimes of solid and solution samples were measured using a conventional laser system. The excitation source was the 355 nm output (third harmonic, 8 ns) of a Spectra-Physics Quanta-Ray Q-switched GCR-150 pulsed Nd-YAG laser (10 Hz). Luminescence decay traces were recorded on a Tektronix Model TDS 620A digital oscilloscope and the lifetime (τ) determination was accomplished by single exponential fitting

of the luminescence decay traces with the model, $I(t) = I_o \exp(-t/\tau)$, where $I(t)$ and I_o stand for the luminescence intensity at time t and 0, respectively. Solution samples for luminescence lifetime measurements were degassed with at least four freeze–pump–thaw cycles. ^{1}H and ^{13}C NMR spectra were recorded on a Bruker DPX-300 (300 MHz) FT-NMR spectrometer, positive-ion FAB mass spectra on a Finnigan MAT95 mass spectrometer and electrospray-ionization mass spectra on a Finnigan LCQ mass spectrometer. Cyclic voltammetric measurements were performed by using a CH Instruments, Inc. model CHI 620 Electrochemical Analyzer. Electrochemical measurements were made in acetonitrile solutions with 0.1 M ^{n}Bu$_4$NPF$_6$ as supporting electrolyte at room temperature. The reference was a Ag–AgNO$_3$ (0.1 M in acetonitrile) electrode and the working electrode glassy carbon (Atomergic Chemetal V25) with a piece of platinum wire as counter electrode in a compartment separated from the working electrode by a sintered glass frit. The ferrocenium–ferrocene couple ($FeCp_2^{+/0}$) was used as the internal reference. All solutions for electrochemical studies were deaerated with pre-purified argon gas just before measurements. Elemental analyses of all the metal complexes were performed on a Carlo Erba 1106 elemental analyzer by the Institute of Chemistry at the Chinese Academy of Sciences in Beijing.

EHMO Calculations

All the calculations were carried out within the standard extended Hückel method[14] with the CACAO program (Version 5.0).[15] The geometrical parameters were based on the X-ray diffraction data. Standard atomic parameters were taken for H, C, O and N.[14b] The exponents (ζ) and the valence shell ionization potential (H_{ii} in eV) used for Ru are the literature parameters,[16] *i.e.* 2.08 and −7.73 for 5s, 2.04 and −4.40 for 5p respectively. The H_{ii} value for 4d was −11.23. A linear combination of two Slater-type orbitals ($\zeta_1 = 5.378$, $c_1 = 0.5340$; $\zeta_2 = 2.303$, $c_2 = 0.6365$) was used to represent the atomic 4d orbitals.

Crystal structure determination

Experimental details are given in Table 1. Crystals of **3** suitable for X-ray studies were obtained by slow diffusion of diethyl ether vapour into an acetonitrile solution of **3**. A red crystal mounted on a glass fiber was used for data collection on a Rigaku AFC7R diffractometer. The space group was determined to be $P\bar{1}$ (no. 2) from statistical analysis of intensity distribution and the successful refinement of the structure solved by Patterson methods and expanded by Fourier methods (PATTY)[17] and refinement by full-matrix least squares using the software package TEXSAN[18] on a Silicon Graphics Indy computer. One crystallographic asymmetric unit consists of one formula unit. The F and O atoms of the anion were disordered with F(1), F(1′), F(1″), F(2), F(2′), F(3) and F(3′) having occupation numbers 0.52, 0.30, 0.18, 0.51, 0.49, 0.60 and 0.40 respectively and O(1), O(1′), O(2), O(2′), O(3) and O(3′) having 0.52, 0.48, 0.58, 0.42, 0.65, and 0.35 respectively. In the least-squares refinement 45 non–H atoms were refined anisotropically, the disordered F and O atoms and C(39) isotropically, the positional parameters of H(1) bonded to N(5) were refined and 27 H atoms at calculated positions with thermal parameters equal to 1.3 times that of the attached C atoms were not refined. The final Fourier difference map was featureless.

Crystals of **4** were obtained by slow diffusion of diethyl ether vapour into an acetonitrile solution of **4**. A purple crystal was used for data collection and the space group determined as above. One crystallographic asymmetric unit consists of half one formula unit. The F atoms of the anion were disordered with F(1), F(2), F(2′), F(3), F(3′), F(4), F(4′), F(5), F(5′), F(6) and F(6′) having occupation numbers 1.0, 0.62, 0.38, 0.60, 0.40, 0.62, 0.38, 0.60, 0.40, 0.60 and 0.40 respectively. In the least-squares refinement 42 non-H atoms were refined anisotropically, 11 disordered F atoms isotropically, and 30 H atoms at calculated positions with thermal parameters equal to 1.3 times that of the attached C atoms were not refined. The final Fourier difference map was featureless.

Crystals of **5** were obtained by slow diffusion of diethyl ether into an acetonitrile solution of **5**. A purple crystal was used for data collection as above. The space group of the crystal was determined to be *C*2/*c* (no. 15) from systematic absences and on the basis of a statistical analysis of intensity distribution and the successful refinement of the structure solved by direct methods (SIR 92)[19] and expanded by Fourier methods and refined by full-matrix least squares using TEXSAN[18] on a Silicon Graphics Indy computer. One crystallographic asymmetric unit consists of one formula unit. S(1) and C(10) were disordered due to rotation of the ring about the C(8)–C(9) bond and S(1′) having occupation number 0.4 was constrained to C(10) having occupation number of 0.6 and C(10′) having occupation number 0.4 was constrained to S(1) having occupation number 0.6. The F and O atoms of the anion were also disordered with F(1), F(1′), F(2), F(2′), F(3), F(3′), O(1), O(1′), O(3) and O(3′) having occupation numbers of 0.58, 0.42, 0.63, 0.37, 0.80, 0.20, 0.68, 0.32, 0.65 and 0.35 respectively. In the least-squares refinement 39 non-H atoms were refined anisotropically, S(1) and C(10) and the 10 disordered F and O atoms and C(33) isotropically, the positional parameters of H(1) bonded to the N(5) and located in the difference Fourier were refined, and 23 other H atoms at calculated positions with thermal parameters equal to 1.3 times that of the attached C atoms were not refined. The 3 H atoms of the disordered thiophene ring were not included in the calculation. The final Fourier difference map was featureless.

CCDC reference numbers 150734–150736.

See http://www.rsc.org/suppdata/dt/b1/b100696g/ for crystallographic data in CIF or other electronic format.

Results and discussion

Synthesis

The synthetic route for the formation of ruthenium(II) orthometallated aminocarbene complexes is summarized in Scheme 1. The terminal acetylene first co-ordinates to the co-ordinatively unsaturated ruthenium(II) metal centre, which rapidly rearranges to form the vinylidene complex. The vinylidene complex cannot be intercepted in the course of the one-pot reaction as the vinylidene ligand is apparently not protected by the planar bipyridine or phenanthroline ligands, making the electron-deficient α-carbon highly susceptible to nucleophilic attack. Thus if a nucleophile, such as aniline, is present, an orthometallated aminocarbene complex is formed readily through the formation of an aminocarbene complex and subsequent orthometallation of the phenyl ring (Scheme 1).[11] However, if water is present, a ruthenium(II) (benzyl)-carbonyl complex is generated instead *via* the hydroxycarbene complex intermediate, which is formed by nucleophilic attack of a water molecule on the α-carbon of the vinylidene ligand (Scheme 2).[11] In a similar reaction studied by Bianchini *et al.*[20] treatment of the vinylidene complexes with primary amines gives thermally unstable ruthenium(II) aminocarbene complexes which degrade *via* toluene elimination. Stable aminocarbene complexes can be obtained only when a secondary amine, such as piperidine, is used instead. On the other hand, in the case studied here, stable orthometallated aminocarbene complexes can be acquired from primary amines. This is probably due to stabilization of the metal centre by fulfilling an octahedral configuration at the expense of orthometallation of the aminophenyl ring. It is also found that only a phenyl ring attached to an amine group can perform orthometallation.

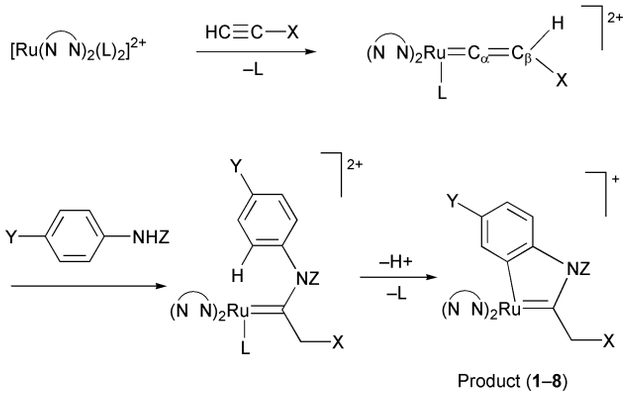

1 N N = bpy, X = Ph, Y = H, Z = H

2 N N = bpy, X = Ph, Y = OMe, Z = H

3 N N = phen, X = Ph, Y = H, Z = H

4 N N = bpy, X = Ph, Y = H, Z = Me

5 N N = bpy, X =  , Y = H, Z = H

6 N N = bpy, X = Ph, Y = Br, Z = H

7 N N = bpy, X = Ph, Y = CF_3, Z = H

8 N N = bpy, X = C_6H_4-Cl-p, Y = H, Z = H

Scheme 1 Synthetic route to ruthenium(II) orthometallated aminocarbenes.

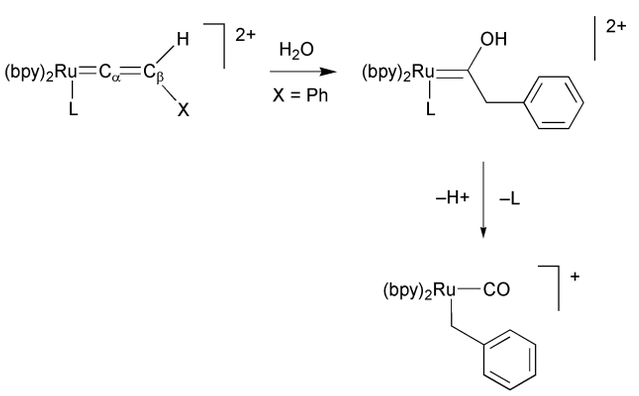

Scheme 2 Synthetic route to ruthenium(II) (benzyl)carbonyl complexes.

This can be accounted for by the lone pair electron delocalization from the nitrogen atom into the phenyl ring, making the *ortho*-carbon electron rich (Scheme 3).

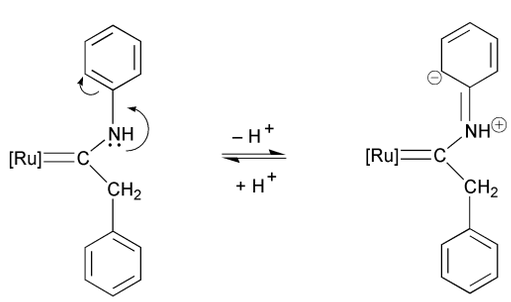

Scheme 3 Lone pair electron delocalization of aminocarbene ligand.

Crystal structure determination

The perspective drawings of the complex cations of **3**–**5** are shown in Figs. 1–3, respectively. Bond distances and angles are in Table 2. In general, all complexes show similar distorted octahedral structures with comparable bond lengths and angles.

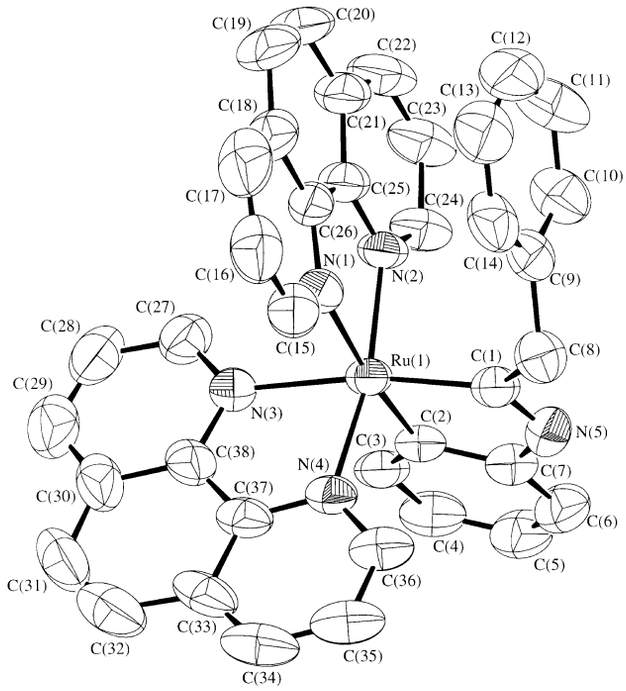

Fig. 1 Perspective drawing of the complex cation of **3** with the atomic numbering scheme. Hydrogen atoms have been omitted for clarity. Thermal ellipsoids are shown at the 40% probability level.

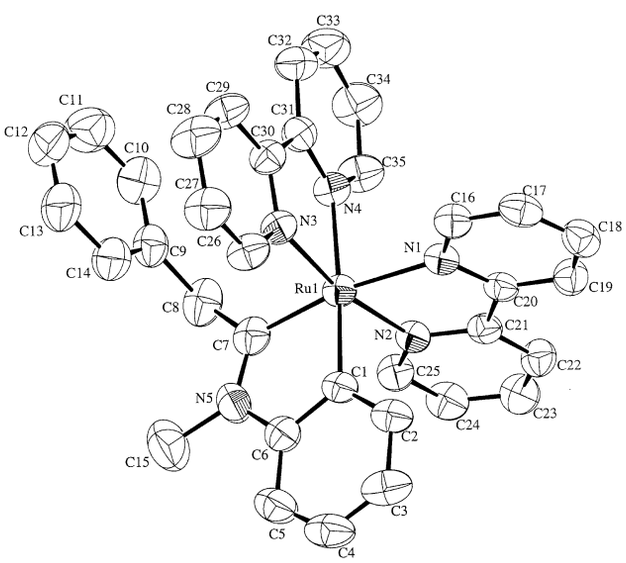

Fig. 2 Perspective drawing of the complex cation of **4**. Details as in Fig. 1.

The N–Ru–N bond angles subtended by the chelating bipyridine ligands vary from 77.1(2) to 77.6(3)° and that by the phenanthroline ligands is 78.6(2)°. This is consistent with the fact that phenanthroline is structurally more rigid than bipyridine. The deviation from the ideal 90° for a regular octahedral geometry is a result of the steric requirements of the bidentate ligands. The C–Ru–C bond angle is in the range 79.6(3)–80.1(4)° comparable to those found in other orthometallated carbene complexes.[21] The bond angles around the carbene carbon range from 114.2(6) to 129.7(5)°, which is consistent with the sp^2 hybridization of the carbene carbon.[21]

The Ru–N bonds [2.051(7)–2.077(4) Å] that are *trans* to the pyridine rings have similar bond lengths to those found in other ruthenium(II) polypyridyl complexes (*ca.* 2.05 Å)[22] but those [2.120(5)–2.155(5) Å] that are *trans* to the orthometallated carbon atoms are longer than normal. This may be accounted for by the strong *trans* effect of the carbon atoms in the orthometallated phenyl rings. In general, the two Ru–C(sp^2) distances

Table 1 Crystal and structure determination data for ruthenium(II) orthometallated aminocarbene complexes **3**–**5**

	3	**4**	**5**
Formula	$[C_{38}H_{28}N_5Ru]^+$ $(CF_3SO_3^-)$	$[C_{35}H_{30}N_5Ru]^+$ (PF_6^-)	$[C_{32}H_{26}N_5RuS]^+$ $(CF_3SO_3^-)$
M_r	804.81	766.69	762.79
T/K	301	301	301
a/Å	12.088(2)	9.851(4)	24.552(7)
b/Å	12.579(3)	12.981(4)	9.855(7)
c/Å	12.820(2)	14.631(4)	30.216(7)
α/°	71.50(1)	70.26(6)	—
β/°	69.34(1)	86.02(6)	116.87(3)
γ/°	88.87(1)	68.59(6)	—
V/Å^3	1720(1)	1636(9)	6521(4)
Crystal colour	Red	Purple	Purple
Crystal system	Triclinic	Triclinic	Monoclinic
Space group	$P\bar{1}$ (no. 2)	$P\bar{1}$ (no. 2)	$C2/c$ (no. 15)
Z	2	2	8
λ/Å (graphite monochromated, Mo-Kα)	0.71073	0.71073	0.71073
μ/cm^{-1}	5.80	5.96	6.68
No. of data collected	5680	6040	6270
No. of unique data	5404	5763	6113
No. of data used in refinement, m	4335	3827	2589
No. of parameters refined, p	465	423	402
R	0.056	0.046	0.052
wR	0.083	0.058	0.065

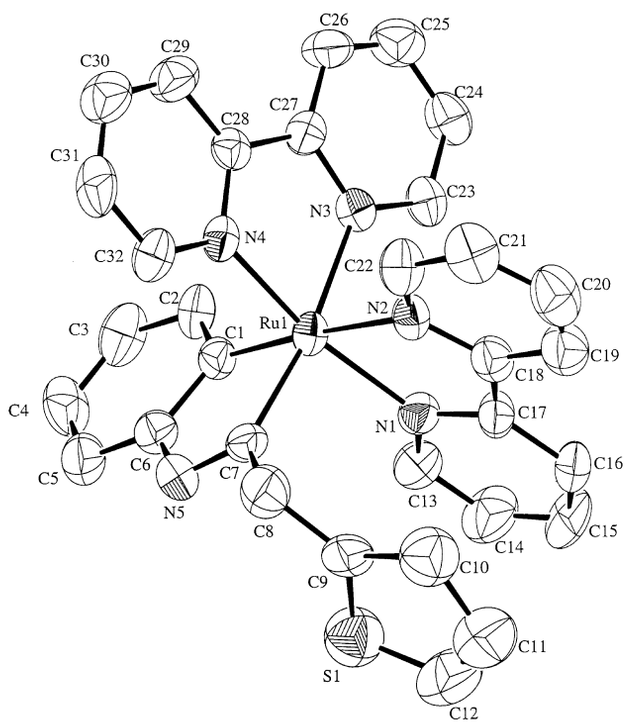

Fig. 3 Perspective drawing of the complex cation of **5**. Details as in Fig. 1.

Table 2 Selected bond distances (Å) and bond angles (deg) for **3**–**5**

3	Ru(1)–N(1)	2.155(5)	Ru(1)–N(2)	2.070(5)
	Ru(1)–N(3)	2.147(5)	Ru(1)–N(4)	2.055(5)
	Ru(1)–C(1)	1.974(6)	Ru(1)–C(2)	2.047(6)
	C(8)–C(9)	1.526(9)	C(1)–C(8)	1.516(9)
	C(1)–N(5)	1.317(8)	C(7)–N(5)	1.417(8)
	N(1)–Ru(1)–N(2)	78.6(2)	N(3)–Ru(1)–N(4)	78.6(2)
	C(1)–Ru(1)–C(2)	79.8(3)	Ru(1)–C(1)–C(8)	129.7(5)
	Ru(1)–C(1)–N(5)	115.9(5)	C(8)–C(1)–N(5)	114.2(6)
4	Ru(1)–N(1)	2.122(5)	Ru(1)–N(2)	2.061(4)
	Ru(1)–N(3)	2.077(4)	Ru(1)–N(4)	2.131(4)
	Ru(1)–C(7)	1.960(7)	Ru(1)–C(1)	2.047(6)
	C(8)–C(9)	1.509(9)	C(7)–C(8)	1.506(9)
	C(7)–N(5)	1.358(8)	C(6)–N(5)	1.421(8)
	C(15)–N(5)	1.479(9)		
	N(1)–Ru(1)–N(2)	77.5(2)	N(3)–Ru(1)–N(4)	77.1(2)
	C(1)–Ru(1)–C(7)	79.6(3)	Ru(1)–C(7)–C(8)	124.8(5)
	Ru(1)–C(7)–N(5)	117.3(5)	C(8)–C(7)–N(5)	117.8(6)
	C(7)–N(5)–C(15)	125.9(7)	C(6)–N(5)–C(7)	115.8(5)
	C(6)–N(5)–C(15)	118.3(6)		
5	Ru(1)–N(1)	2.074(7)	Ru(1)–N(2)	2.128(7)
	Ru(1)–N(3)	2.138(7)	Ru(1)–N(4)	2.051(7)
	Ru(1)–C(7)	1.963(9)	Ru(1)–C(1)	2.053(9)
	C(8)–C(9)	1.51(1)	C(7)–C(8)	1.50(1)
	C(7)–N(5)	1.33(1)	C(6)–N(5)	1.40(1)
	N(1)–Ru(1)–N(2)	77.6(3)	N(3)–Ru–N(4)	77.6(3)
	C(1)–Ru(1)–C(7)	80.1(4)	Ru(1)–C(7)–C(8)	128.7(8)
	Ru(1)–C(7)–N(5)	115.7(7)	C(8)–C(7)–N(5)	115.7(8)

are significantly different. The bond distances from ruthenium to the carbene carbon [1.960(7)–1.974(6) Å] are shorter than that of ruthenium to the metallated phenyl ring [2.047(6)–2.053(9) Å]. This can be ascribed to the presence of double bond character in the ruthenium to carbene carbon bonds. A substantial double-bond character is noticed between the heteroatom and the carbene carbon. The C–N bond distances [1.317(8)–1.358(8) Å] are reduced below that characteristic of a single bond between N and an sp^2 hybridized carbon, which is typical of Fischer type aminocarbenes (*ca.* 1.31 Å).[23]

For complex **4** the carbene carbon to nitrogen bond [C(7)–N(5), 1.358(8) Å] is significantly longer than those observed in the other complexes [1.317(8)–1.33(1) Å]. The bond angles around the nitrogen atom [125.9(7), 118.3(6) and 115.8(5)°] show that the nitrogen atom is sp^2 hybridized. The Ru(1)–C(7)–C(8) bond angle is *ca.* 4° larger and the C(8)–C(7)–N(5) bond angle *ca.* 4° smaller than those found in other complexes. All these can be ascribed to the presence of the *N*-methyl group, which increases the steric bulkiness around the nitrogen atom. The bond lengths around the nitrogen atom are in the decreasing order of C(15)–N(5), C(6)–N(5) and C(7)–N(5), showing the increasing C–N double bond character.

All ruthenium(II) orthometallated aminocarbene complexes show π–π interactions between the phenyl ring in the phenylmethylene group and the pyridyl ring in the ancillary ligand of bpy or phen. The distances observed between the two aromatic rings in **2**, **3**, **4** and **5** are 3.58, 3.45, 3.55 and 3.62 Å, respectively. The dihedral angles between the two planes are 10.31, 12.96,

Table 3 Calculated molecular orbital energies and transition energies

Complex	No.	Level/eV	Ru	Composition (%) Ancillary ligands [2(bpy) or 2(phen)]	Composition (%) Orthometallated aminocarbene ligand	HOMO–LUMO Energy gap, ΔE_{gap}/eV
2[a]	97	−8.892	5	47	42	1.275
	98	−9.530	7	88	—[b]	(100 ⟶ 99)
	99 (LUMO)	−9.658	2	89	1	
	100 (HOMO)	−10.933	85	—[b]	6	
	101	−11.002	78	8	5	
	102	−11.259	73	6	14	
3	101	−9.434	—[b]	94	1	1.251
	102	−9.593	10	90	—[b]	(104 ⟶ 103)
	103 (LUMO)	−9.686	1	94	1	
	104 (HOMO)	−10.937	86	3	6	
	105	−11.029	77	12	5	
	106	−11.239	74	5	16	
4	96	−8.965	9	18	61	1.284
	97	−9.548	9	87	—[b]	(99 ⟶ 98)
	98 (LUMO)	−9.654	1	91	1	
	99 (HOMO)	−10.938	85	1	4	
	100	−11.010	77	10	5	
	101	−11.284	73	3	16	

[a] Crystal structural data taken from reference 11. [b] Percentage composition of less than 0.5%.

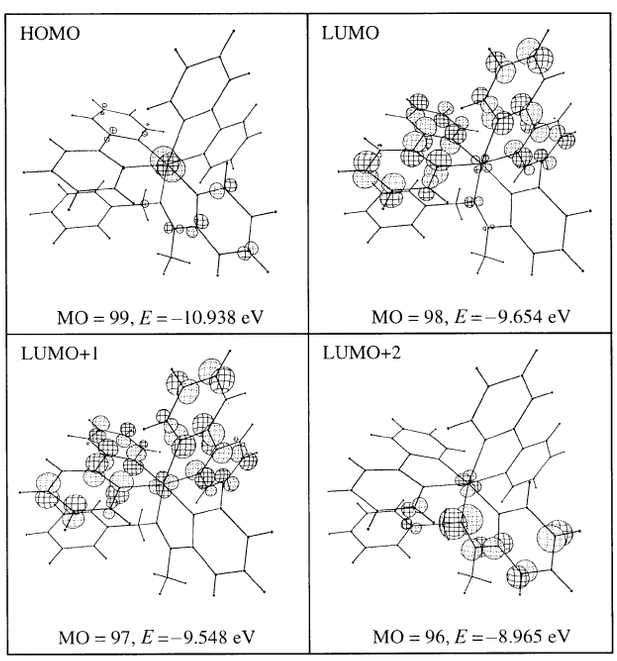

Fig. 4 CACAO plots of HOMO, LUMO, LUMO+1 and LUMO+2 of **4**. The minimum wavefunction coefficient is 0.12.

11.65 and 12.51° correspondingly. The short distances and the nearly parallel structures imply the presence of π–π interaction, which is weakest for **5**. This may be explained by the poor π–π overlap between the five-membered thiophene ring and six-membered pyridyl ring.

EHMO Calculations

Table 3 summarizes the calculated molecular orbital energies, percentage composition and the HOMO–LUMO energy gap of **2**, **3** and **4**. Fig. 4 shows the CACAO plots of HOMO, LUMO, LUMO+1 and LUMO+2 of **4**. From the calculations the energy gaps between the HOMO and the LUMO of different complexes were small. However, it is important to stress that the qualitative results concerning the nature of the frontier orbitals are more meaningful while the quantitative results are not important in such semi-empirical MO studies. The HOMO was found to contain predominantly ruthenium metal centre character (≥85%) with some partial localization on the aminocarbene ligand. The energies of the LUMO and LUMO+1 are nearly the same, and are mainly localized on the ancillary ligands of bipyridine or phenanthroline (≥87%). The LUMO+2 was made up of orthometallated aminocarbene π* orbital character for **2** (42%) and **4** (61%), and phenanthroline π* orbital character for **3** (94%). The assignment of LUMO+2 in **3** is suggestive of the presence of lower lying π* orbitals in the more delocalized phenanthroline ligands.

Electronic absorption spectroscopy

All the ruthenium(II) aminocarbene complexes are soluble in common organic solvents to give deep purplish red solutions. They show intense absorption bands in the UV region and moderately intense absorption bands in the visible region. All complexes have essentially identical absorption spectra. The electronic absorption bands of all complexes at wavelengths smaller than 300 nm have large molar absorption coefficients which are of the order of 10^4 dm^3 mol^{-1} cm^{-1}. These absorption bands most probably arise from the intraligand (IL) π ⟶ π* transitions localized on phenyl rings and ancillary ligands such as bipyridine and phenanthroline. The absorption bands at 464–480 nm are tentatively assigned to the dπ(Ru) ⟶ π*(aminocarbene) MLCT transitions, and those at 564–576 nm mainly due to the π(Ru) ⟶ π*(diimine) MLCT transitions, probably with some mixing of a π(aminocarbene) ⟶ π*(diimine) ligand-to-ligand charge transfer (LL′CT) character.

Emission properties

Excitation of all complexes at $\lambda > 350$ nm produces red luminescence (Table 4). All ruthenium(II) orthometallated aminocarbene complexes show emission bands at 782–813 nm. A change in the substituents on the aminocarbene ligands has been shown to have relatively little influence on the emission energies of these complexes. It is likely that the emission originates from the lowest energy triplet metal-to-ligand charge transfer (MLCT) state, probably derived from the excitation

Table 4 Photophysical data for the ruthenium(II) orthometallated aminocarbene complexes

Complex	Medium (T/K)	Emission λ_{em}[a]/nm (τ_0/μs)	Absorption λ_{abs}[b]/nm (ε/dm^3 mol^{-1} cm^{-1})
1[c]	CH_3CN (298)	808 (<0.1)	250 (37960), 298 (46400), 370 (11630), 484 (6230), 572 (6610)
	Solid (298)	775	
	Solid (77)	704	
	Glass[d] (77)	742	
2[c]	CH_3CN (298)	813 (<0.1)	250 (37680), 298 (52720), 370 (12650), 482 (6850), 571 (7090)
	Solid (298)	767	
	Solid (77)	701	
	Glass[d] (77)	745	
3	CH_3CN (298)	804 (<0.1)	226 (89810), 266 (91270), 352 (5040), 464 (7830), 564 (6600)
	Solid (298)	774	
	Solid (77)	704	
	Glass[d] (77)	743	
4	CH_3CN (298)	806 (<0.1)	248 (43020), 290 sh (46840), 298 (55540), 374 (14690), 482 (8040), 576 (8270)
	Solid (298)	777	
	Solid (77)	713	
	Glass[d] (77)	743	
5	CH_3CN (298)	806 (<0.1)	248 (36470), 288 sh (40730), 296 (44440), 368 (11010), 476 (6000), 564 (6200)
	Solid (298)	776	
	Solid (77)	708	
	Glass[d] (77)	744	
6	CH_3CN (298)	792 (<0.1)	250 (36300), 296 (45310), 366 (11390), 470 (6610), 554 (6960)
	Solid (298)	754	
	Solid (77)	685	
	Glass[d] (77)	706	
7	CH_3CN (298)	782 (<0.1)	248 (36870), 296, (42410), 368 (9660), 464 (5740), 550 (6140)
	Solid (298)	740	
	Solid (77)	700	
	Glass[d] (77)	700	
8	CH_3CN (298)	809 (<0.1)	250 (40540), 298 (50920), 370 (12800), 488 (6700), 570 (7560)
	Solid (298)	776	
	Solid (77)	705	
	Glass[d] (77)	736	

[a] Excitation wavelength at 580 nm. Emission maxima are corrected values. [b] In acetonitrile at 298 K. [c] From reference 11. [d] EtOH–MeOH (4 : 1, v/v).

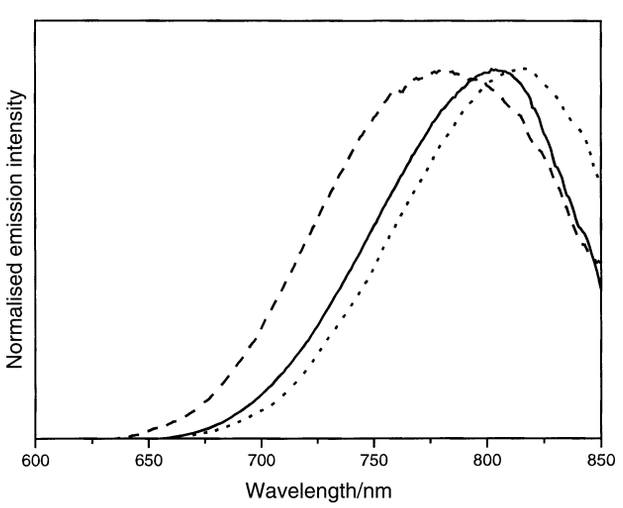

Fig. 5 Normalized solution emission spectra of **2** (···), **3** (–) and **7** (- -) in acetonitrile at 298 K.

involving a dπ(Ru) to π*(bpy/phen) MLCT transition. A small energy dependence in the emission energy in the order **7** > **6** > **1** ≈ **5** ≈ **4** ≈ **8** > **2** is observed, which appears to be in line with such a ^{3}MLCT assignment. The slightly lower ^{3}MLCT transition energy of **2** than **1** is probably due to the larger electron donating ability as well as the poorer π-accepting ability of the methoxy-substituted orthometallated aminocarbene ligand, rendering the dπ(Ru) orbital slightly higher in energy. Similarly, the blue shifts of the ^{3}MLCT emission of **6** and **7** than **1** and **2** (Fig. 5) may be rationalized by the presence of the respective electron withdrawing bromo and trifluoromethyl substituents on the orthometallated aminocarbene moiety in **6** and **7**, which lowers the dπ(Ru) orbital energy. The ^{3}MLCT emission energy was found to correlate well with the electronic effects of the orthometallated aminocarbene ligands, in which the presence of the most electron-rich methoxy group in **2** shows the lowest emission energy, while the presence of the most electron-poor trifluoromethyl group in **7** shows the highest ^{3}MLCT emission energy. The emission bands are also found to be of much lower energies than that of $[Ru(bpy)_3]^{2+}$ (613 nm),[24] which can be explained by the electron-donating ability of the orthometallated phenyl rings as well as the poorer π-accepting ability of the orthometallated aminocarbene moiety than 2,2′-bipyridine, resulting in the formation of a higher-lying dπ(Ru) orbital. The assignments have also been supported by results obtained from EHMO studies, in which a small difference in the HOMO-LUMO gap energy between complexes with different substituents on the aminocarbene ligands has been observed.

Electrochemical properties

The electrochemical data for complexes **1**–**8** are collected in Table 5. In general, the changes in reduction and oxidation potentials are probably due to the relative stabilization of the ruthenium(II) state over Ru(III) by a combination of σ and π effects exhibited by the ligands. All the ruthenium(II) orthometallated aminocarbene complexes show similar reversible to quasi-reversible couples at *ca.* −1.6 and −1.9 V *vs.* SCE. These potentials are relatively independent of the scan rate. ΔE_p values of *ca.* 60–90 mV were observed ($\Delta E_p = |E_{pa} - E_{pc}|$). These couples are assigned to the one-electron bipyridine-based reductions that are commonly observed in other ruthenium(II) bipyridine complexes.[25] The first reduction occurs at a more negative potential than that found in $[Ru(bpy)_3]^{2+}$ (−1.33 V *vs.*

Table 5 Electrochemical data for ruthenium(II) orthometallated aminocarbene complexes[a]

Complex	Oxidation[b]/V *vs.* SCE	Reduction[c]/V *vs.* SCE
1[d]	+1.66	−1.66
		−1.89
2[d]	+1.67	−1.65
		−1.88
3	+1.67	−1.66
		−1.89
4	+1.67	−1.65
		−1.87
5	+1.73	−1.66
		−1.86
6	+1.77	−1.63
		−1.87
7	+1.86	−1.58
		−1.80
8	+1.65	−1.65
		−1.86

[a] In acetonitrile solution with 0.1 M $^{n}Bu_4NPF_6$ as supporting electrolyte at room temperature; scan rate 100 mV s^{-1}. [b] E_{pa} refers to the anodic peak potential for the irreversible oxidation waves. [c] $E_{1/2} = (E_{pa} + E_{pc})/2$; E_{pa} and E_{pc} are the anodic and cathodic peak potentials, respectively. [d] From reference 11.

SCE).[25] This indicates that the bipyridine ligands in the orthometallated aminocarbene complexes are poorer π acceptors, which can be ascribed to the charge effect as well as the better electron-donating and poorer π-accepting abilities of the orthometallated phenyl ligands, enhancing the dπ(Ru) ⟶ π*(bpy) π back donation. Irreversible oxidation waves are noted at *ca.* +1.6 to +1.9 V *vs.* SCE and are assigned as metal-centred oxidation from Ru(II) to Ru(III). The irreversible nature of the oxidation is indicative of the instability of the ruthenium aminocarbene complexes, in which the HOMO is not purely metal-centred in character, but with some localization on the aminocarbene ligand. The oxidations of ruthenium(II) in **6** and **7** are slightly more difficult. This may be ascribed to the presence of electron withdrawing groups on the orthometallated aminocarbene ligands, which results in the formation of lower lying dπ(Ru) orbitals.

Acknowledgements

V. W.-W. Y. acknowledges financial support from the Research Grants Council and The University of Hong Kong, B. W.-K. C. the receipt of a Research Associateship from the Setting-Up Grant supported by the Vice-Chancellor's Development Fund of The University of Hong Kong, and C.-C. K. the receipt of a postgraduate studentship (1999–2000) from The University of Hong Kong and a Croucher Scholarship (2000–2001) from the Croucher Foundation.

References

1 (*a*) H. Nishiyama, Y. Itoh, J. Matsumoto, S. B. Park and K. Itoh, *J. Am. Chem. Soc.*, 1994, **116**, 2223; (*b*) S. B. Park, H. Nishiyama, Y. Itoh and K. Itoh, *J. Chem. Soc., Chem. Commun.*, 1994, 1325; (*c*) B. Çetinkaya, I. Özdemir and P. H. Dixneuf, *J. Organomet. Chem.*, 1997, **534**, 153; (*d*) W. C. Lo, C. M. Che, K. F. Cheng and T. C. W. Mak, *Chem. Commun.*, 1997, 1205.

2 W. A. Herrmann and C. Köcher, *Angew. Chem., Int. Ed. Engl.*, 1997, **118**, 100; T. Weskamp, W. C. Schattenmann, M. Spiegler and W. A. Herrmann, *Angew. Chem., Int. Ed.*, 1998, **37**, 2490; D. M. Lynn, B. Mohr, R. H. Grubbs, L. M. Henling and M. W. Day, *J. Am. Chem. Soc.*, 2000, **122**, 6601; K. J. Ivin and J. C. Mol, *Olefin Metathesis and Metathesis Polymerization*, Academic Press, London, 1997; T. R. Belderrain and R. H. Grubbs, *Organometallics*, 1997, **16**, 4001; B. Mohr, M. Weck, J. P. Sauvage and R. H. Grubbs, *Angew. Chem., Int. Ed. Engl.*, 1997, **36**, 1308; E. L. Dias, S. T. Nguyen and R. H. Grubbs, *J. Am. Chem. Soc.*, 1997, **119**, 3887.

3 R. H. Grubbs, *Comprehensive Organometallic Chemistry*, Pergamon, New York, 1982, vol. 8, p. 499; S. T. Nguyen, L. K. Johnson and R. H. Grubbs, *J. Am. Chem. Soc.*, 1992, **114**, 3974; D. M. Lynn, S. Kanaoka and R. H. Grubbs, *J. Am. Chem. Soc.*, 1996, **118**, 784; P. Schwab, R. H. Grubbs and J. W. Ziller, *J. Am. Chem. Soc.*, 1996, **118**, 100; D. M. Lynn, B. Mohr and R. H. Grubbs, *J. Am. Chem. Soc.*, 1998, **120**, 1627.

4 R. H. Grubbs, S. J. Miller and G. C. Fu, *Acc. Chem. Res.*, 1995, **28**, 446; S. T. Nguyen and R. H. Grubbs, *J. Am. Chem. Soc.*, 1993, **115**, 9858; M. A. Hillmyer, W. R. Laredo and R. H. Grubbs, *Macromolecules*, 1995, **28**, 6311; P. Schwab, R. H. Grubbs and J. W. Ziller, *J. Am. Chem. Soc.*, 1996, **118**, 100; Z. Wu, A. D. Benedicto and R. H. Grubbs, *Macromolecules*, 1993, **26**, 4975; S. T. Nguyen, L. K. Hohnson, R. H. Grubbs and J. W. Ziller, *J. Am. Chem. Soc.*, 1992, **114**, 3974; D. M. Lynn, S. Kanaoka and R. H. Grubbs, *J. Am. Chem. Soc.*, 1996, **118**, 784; C. Fraser and R. H. Grubbs, *Macromolecules*, 1995, **28**, 7248; M. A. Hillmyer, A. D. Benedicto, S. T. Nguyen, Z. Wu and R. H. Grubbs, *Macromol. Symp.*, 1995, 441; S. Kanaoka and R. H. Grubbs, *Macromolecules*, 1995, **28**, 4707; A. Demonceau, A. F. Noels, E. Saive and A. J. Habert, *J. Mol. Catal.*, 1992, **76**, 123; M. Weck, P. Schwab and R. H. Grubbs, *Macromolecules*, 1996, **29**, 1789; G. C. Fu, S. T. Nguyen and R. H. Grubbs, *J. Am. Chem. Soc.*, 1993, **115**, 9856; S. J. Miller, S. H. Kim, Z. R. Chen and R. H. Grubbs, *J. Am. Chem. Soc.*, 1995, **117**, 2108; S. J. Miller and R. H. Grubbs, *J. Am. Chem. Soc.*, 1995, **117**, 5855; S. H. Kim, N. Bowden and R. H. Grubbs, *J. Am. Chem. Soc.*, 1994, **116**, 10801.

5 G. C. Fu and R. H. Grubbs, *J. Am. Chem. Soc.*, 1993, **115**, 3800; O. Fujimura, G. C. Fu and R. H. Grubbs, *J. Org. Chem.*, 1994, **59**, 4029.

6 F. Fischer and H. Tropsch, *Chem. Ber.*, 1923, **56**, 2428; F. Fischer and H. Tropsch, *Chem. Ber.*, 1926, **59**, 830; M. L. Turner, H. C. Long, A. Shenton, P. K. Byers and P. M. Maitlis, *Chem. Eur. J.*, 1995, **1**, 549.

7 See, for example: P. González-Herrero, B. Weberndörfer, K. Ilg, J. Wolf and H. Werner, *Angew. Chem., Int. Ed.*, 2000, **39**, 18; M. C. Puerta and P. Valerga, *Coord. Chem. Rev.*, 1999, **195**, 977, and references therein; B. Mohr, D. M. Lynn and R. H. Grubbs, *Organometallics*, 1996, **15**, 4317; Z. Atherton, C. W. Faulkner, S. L. Ingham, A. K. Kakkar, M. S. Khan, J. Lewis, N. J. Long and P. R. Raithby, *J. Organomet. Chem.*, 1996, **462**, 265; T. Braun, P. Steinert and H. Werner, *J. Organomet. Chem.*, 1995, **488**, 169; D. Touchard, C. Morice, V. Cadierno, P. Haquette, L. Toupet and P. H. Dixneuf, *Organometallics*, 1994, **13**, 5030; M. P. Gamasa, J. Gimeno, B. M. Martín-vaca, J. Borge, S. García-Granda and E. Perez-Carreño, *Organometallics*, 1994, **13**, 4045; P. H. Dixneuf, D. Touchard, P. Haquette, N. Pirio and L. Toupet, *Organometallics*, 1993, **12**, 3132; Y. Sun, N. J. Taylor and A. J. Carty, *J. Organomet. Chem.*, 1992, **423**, C43; G. Jia, J. C. Gallucci, A. L. Rheingold, B. S. Haggerty and D. W. Meek, *Organometallics*, 1991, **10**, 3459; M. I. Bruce and R. C. Wallis, *J. Organomet. Chem.*, 1978, **161**, C1.

8 See, for example: C. Bianchini and H. M. Lee, *Organometallics*, 2000, **19**, 1833; C. Gemel, J. C. Huffman, K. G. Caulton, K. Mauthner and K. Kirchner, *J. Organomet. Chem.*, 2000, **594**, 342; B. Buriez, I. D. Burns, A. F. Hill, A. J. P. White, D. J. Williams and J. D. E. T. Wilton-Ely, *Organometallics*, 1999, **18**, 1504; I. del Río, R. A. Gossage, M. S. Hannu, M. Lutz, A. L. Spek and G. van Koten, *Organometallics*, 1999, **18**, 1097; A. Klose, E. Solari, J. Hesschenbrouck and C. Floriani, *Organometallics*, 1999, **18**, 360; Y. Zhu, O. Clot, M. O. Wolf and G. P. A. Yap, *J. Am. Chem. Soc.*, 1998, **120**, 1812; A. Klose, E. Solari, C. Floriani, S. Geremia and L. Randaccio, *Angew. Chem., Int. Ed.*, 1998, **37**, 148; M. S. Sanford, L. M. Henling and R. H. Grubbs, *Organometallics*, 1998, **17**, 5384; C. Gemel, G. Kickelbick, R. Schimid and K. Kirchner, *J. Chem. Soc., Dalton Trans.*, 1997, 5406; C. Slugovc, V. N. Sapunov, P. Wiede, K. Mereiter, R. Schmid and K. Kirchner, *J. Chem. Soc., Dalton Trans.*, 1997, 4209; C. M. Che, S. M. Yang, M. C. W. Chan, K. K. Cheung and S. M. Peng, *Organometallics*, 1997, **16**, 2819; A. Pedersen, M. Tilset, K. Folting and K. G. Caulton, *Organometallics*, 1995, **14**, 875; T. Rappert and A. Yamamoto, *Organometallics*, 1994, **13**, 4984; M. A. Esteruelas, A. Miguel, F. J. Lahoz, A. M. Lopez, E. Onate and L. A. Oro, *Organometallics*, 1994, **13**, 1669; J. Montoya, A. Santos, J. Lopez, A. M. Echavarren, J. Ros and A. Romero, *J. Organomet. Chem.*, 1992, **426**, 383; A. M. Echavarren, J. Lopez, A. Santos, A. Romero, J. A. Hermoso and A. Vegas, *Organometallics*, 1991, **10**, 2371; Y. Degani and T. Willner, *J. Chem. Soc., Chem. Commun.*, 1985, 648.

9 V. Balzani and F. Scandola, *Supramolecular Photochemistry*, Ellis Horwood, London, 1991; K. Kalyanasundaram, *Photochemistry of Polypyridine and Porphyrin Complexes*, Academic Press, London, 1992.

10 V. W. W. Yam, K. L. Yu and K. K. Cheung, *J. Chem. Soc.*, *Dalton Trans.*, 1999, 2913; V. W. W. Yam and K. K. W. Lo, *Chem. Soc. Rev.*, 1999, **28**, 323; V. W. W. Yam, K. K. W. Lo and K. M. C. Wong, *J. Organomet. Chem.*, 1999, **578**, 3; V. W. W. Yam, S. H. F. Chong and K. K. Cheung, *Chem. Commun.*, 1998, 2121; V. W. W. Yam, K. K. W. Lo, W. K. M. Fung and C. R. Wang, *Coord. Chem. Rev.*, 1998, **171**, 17; V. W. W. Yam, W. K. M. Fung, K. M. C. Wong and V. C. Y. Lau, *Chem. Commun.*, 1998, 777; V. W. W. Yam, V. W. M. Lee and K. K. Cheung, *Organometallics*, 1997, **16**, 2833; V. W. W. Yam, V. W. M. Lee and K. K. Cheung, *J. Chem. Soc.*, *Chem. Commun.*, 1994, 2075.
11 V. W. W. Yam, B. W. K. Chu and K. K. Cheung, *Chem. Commun.*, 1998, 2261.
12 T. B. Patrick, J. M. Disher and W. J. Probst, *J. Org. Chem.*, 1972, **37**, 4467.
13 B. P. Sullivan, D. J. Salmon and T. J. Meyer, *Inorg. Chem.*, 1978, **17**, 3334.
14 (*a*) R. Hoffmann and W. N. Lipscomb, *J. Chem. Phys.*, 1962, **36**, 2179; (*b*) R. Hoffmann, *J. Chem. Phys.*, 1963, **39**, 1397.
15 C. Mealli and D. M. Proserpio, *J. Chem. Educ.*, 1990, **67**, 399.
16 R. Hoffmann and K. Tatsumi, *J. Am. Chem. Soc.*, 1981, **103**, 3328.
17 PATTY: P. T. Beurskens, G. Admiraal, G. Beurskens, W. P. Bosman, S. Garcia-Granda, R. O. Gould, J. M. M. Smits and C. Smykalla, The DIRDIF program system, Technical Report of the Crystallography Laboratory, University of Nijmegen, 1992.
18 TeXsan, Crystal Structure Analysis Package, Molecular Structure Corp., Houston, TX, 1985, 1992.
19 SIR 92, A. Altomare, M. Cascarano, C. Giacovazzo, A. Guagliardi, M. C. Burla, G. Polidori and M. Cammalli, *J. Appl. Crystallogr.*, 1994, **27**, 435.
20 C. Bianchini, J. A. Casares, M. Peruzzini, A. Romerosa and F. Zanobini, *J. Am. Chem. Soc.*, 1996, **118**, 4585; C. Bianchini, G. Purches, F. Zanobini and M. Peruzzini, *Inorg. Chim. Acta*, 1998, **272**, 1; C. Bianchini, D. Masi, A. Romerosa, F. Zanobini and M. Peruzzini, *Organometallics*, 1999, **18**, 2376.
21 P. B. Hitchcock, M. F. Lappert and P. L. Pye, *J. Chem. Soc.*, *Dalton Trans.*, 1978, 826.
22 D. Schomburg, S. Neumann and R. Schmutzler, *J. Chem. Soc.*, *Chem. Commun.*, 1979, 848.
23 F. A. Cotton and C. M. Lukehart, *Prog. Inorg. Chem.*, 1972, **16**, 487.
24 J. N. Demas and G. A. Crosby, *J. Am. Chem. Soc.*, 1971, **93**, 2841; A. J. Juris, V. Balzani, P. Belser and A. von Zelewsky, *Helv. Chim. Acta*, 1981, **64**, 2175; K. Kalyanasundaram, *Coord. Chem. Rev.*, 1982, **46**, 159, and references therein.
25 N. E. Tokel-Takvoryan, R. E. Hemingway and A. J. Bard, *J. Am. Chem. Soc.*, 1973, **95**, 6582.